PRECIPITATION OF A CLOUD OF SUSPENDED PARTICLES ON A HORIZONTAL SURFACE

G. M. Makhviladze and O. I. Melikhov

UDC 532.529

Numerical studies of the process of gravitational precipitation of a cloud of suspended particles onto a plane horizontal surface were carried out in [1, 2], assuming plane symmetry. Both the motion of the cloud far from the surface (in an infinite medium), as well as the precipitation of particles on the surface were studied in detail. In [3] the descent of a spherical cloud of monodispersed particles in an infinite incompressible fluid was studied numerically, assuming axial symmetry. It is evident from the results of [1-3] that despite the different geometry the motion of the cloud in an infinite medium is qualitatively the same in the two cases. A cylindrical cloud separates into two symmetric parts, while a spherical cloud transforms into a ring. In both cases vortex motion is induced in the carrier medium.

On the basis of the equations of the mechanics of a multiphase medium [4] we study numerically the precipitation of a cloud of suspended particles on a horizontal surface in both the plane and axisymmetric cases. A detailed comparison of these two cases is given.

1. We consider a gas at temperature T_0 in static equilibrium in the field of gravity. At the initial instant of time there is a cloud of solid, monodispersed spherical particles at a height H_0 above a plane horizontal surface. The cloud is initially at rest. We consider a cylindrical cloud whose axis is parallel to the horizontal surface (plane symmetry with the symmetry parameter $\nu = 0$) or a spherical cloud (axisymmetric problem, $\nu = 1$). We use the plane-symmetric or axisymmetric equations of motion in these two cases. Let r be the radial cylindrical coordinate or the horizontal Cartesian coordinate, and let z be the vertical coordinate, directed oppositely to the field of gravity, where z = 0 is the plane of precipitation. Then the initial conditions can be written as

$$t = 0:\ \mathbf{U}_1 = \mathbf{U}_2 = 0,\ \rho_1 = \rho_{10}\exp(-gz/R_0T_0),$$
$$n = n_0\exp[-(r^2 + (z - H_0)^2)/R^2], \qquad (1.1)$$
$$\rho_2 = \rho_2^0 n\pi d^3/6,\quad p = R_0\rho_1 T_0.$$

Here the indices 1 and 2 refer to the gas and particles, respectively; t is the time; $\mathbf{U}_i(u_i, v_i)$, ρ_i (i = 1.2) is the average velocity and density of the phases; n is the concentration of particles; g is the acceleration of gravity; R_0 is the universal gas constant; $\rho_2{}^0$ and d are the intrinsic density and diameter of a particle; ρ_{10} is the initial density of the gas near the surface of precipitation H_0 and R are the initial height of the cloud and its radius; p is the pressure of the gas, which is assumed to be ideal; n_0 is the maximum concentration of particles to t = 0.

We consider a suspension with a small volume fraction of particles ($\lesssim 10^{-3}$), which means that we can neglect collisions between the particles and also the total volume of the particles. Fragmentation and evaporation of particles are insignificant, and are not considered here. Heating of the medium due to viscous dissipation of energy is small, and therefore the precipitation can be assumed to be an isothermal process. Hence the temperature of the gas and particles remains constant at the initial value T_0.

The plane or axisymmetric motion of the suspension is described by the following equations, written in terms of dimensionless variables:

$$\frac{d_1\rho_1}{dt} = -\rho_1\left(\frac{\partial u_1}{\partial r} + \frac{\partial v_1}{\partial z}\right) - \frac{\nu\rho_1 u_1}{r},\quad p = \rho_1, \qquad (1.2)$$
$$\rho_1\frac{d_1u_1}{dt} = -\mathrm{Eu}\frac{\partial p}{\partial r} + \frac{1}{\mathrm{Re}}\left[\frac{4}{3}\frac{\partial^2 u_1}{\partial r^2} + \frac{\partial^2 u_1}{\partial z^2} + \frac{1}{3}\frac{\partial^2 v_1}{\partial r\,\partial z} + \frac{4}{3}\nu\left(\frac{1}{r}\frac{\partial u_1}{\partial r} - \frac{u_1}{r^2}\right)\right] - f_r,$$

Moscow. Translated from Zhurnal Prikladnoi Mekhaniki i Tekhnicheskoi Fiziki, No. 2, pp. 97-101, March-April, 1987. Original article submitted February 6, 1986.

0021-8944/87/2802-0253$12.50

$$\rho_1 \frac{d_1 v_1}{dt} = -\mathrm{Eu}\frac{\partial p}{\partial z} - \rho_1 + \frac{1}{\mathrm{Re}}\left[\frac{\partial^2 v_1}{\partial r^2} + \frac{4}{3}\frac{\partial^2 v_1}{\partial z^2} + \frac{1}{3}\frac{\partial^2 u_1}{\partial r\,\partial z} + \frac{v}{r}\left(\frac{\partial v_1}{\partial r} + \frac{1}{3}\frac{\partial u_1}{\partial z}\right)\right] - f_z;$$

$$\frac{d_2\rho_2}{dt} = -\rho_2\left(\frac{\partial u_2}{\partial r} + \frac{\partial v_2}{\partial z}\right) - \frac{v\rho_2 u_2}{r}, \quad \rho_2\frac{d_2 u_2}{dt} = f_r, \quad \rho_2\frac{d_2 v_2}{dt} = -\rho_2 + f_z; \tag{1.3}$$

$$\frac{d_i}{dt} \equiv \frac{\partial}{\partial t} + u_i\frac{\partial}{\partial r} + v_i\frac{\partial}{\partial z}, \quad \mathrm{Eu} = R_0 T_0/Rg, \quad \mathrm{Re} = R\sqrt{Rg}\,\rho_{10}/\eta, \tag{1.4}$$

where we use characteristic scales of length, time, velocity, density, pressure, and concentration given by R, $\sqrt{R/g}$, $\sqrt{Rg}$, ρ_{10}, $R_0\rho_{10}T_0$, n_0; Eu and Re are the Euler and Reynolds numbers; η is the dynamical viscosity. The exchange term $f(f_r, f_z)$ describes the interaction between the two phases and has the form

$$\mathbf{f} = \rho_1\rho_2\left(1 + 0{,}158\,\mathrm{Re}_p^{2/3}\right)(\mathbf{U}_1 - \mathbf{U}_2)/\tau_r,$$
$$\mathrm{Re}_p = \mathrm{Re}_p^0\rho_1|\mathbf{U}_1 - \mathbf{U}_2|, \quad \mathrm{Re}_p^0 = d\sqrt{Rg}\,\rho_{10}/\eta, \quad \tau_r = \rho_2^0 d^2/18\eta\sqrt{Rg}. \tag{1.5}$$

Here Re_p is the instantaneous Reynolds number of a particle; Re_p^0 is the Reynolds number of a particle constructed from the characteristic velocity of convection; τ_r is the dimensionless velocity relaxation time of the particles, calculated in the Stokes approximation. In (1.5) we have used an empirical relation between the drag coefficient of a particle and its Reynolds number which closely approximates the experimental curve in the region $0 \le \mathrm{Re}_p \le 700$. Here we consider instantaneous Reynolds numbers of order 10^2, which fall outside of the region of applicability of Stokes' law. Therefore the relaxation time is several times smaller than τ_r.

The boundary conditions take into account the symmetry of the problem with respect to the plane (or the axis) r = 0, static equilibrium of the gas at infinity and the "no-slip" condition of the gas at the surface of precipitation:

$$r = 0\colon\ u_1 = u_2 = 0,\ \partial v_1/\partial r = 0,\ \partial\rho_1/\partial r = 0;$$
$$r^2 + z^2 \to \infty\colon\ \mathbf{U}_1 = 0,\ \partial p/\partial z = -\rho_1/\mathrm{Eu};\ z = 0\colon\ \mathbf{U}_1 = 0. \tag{1.6}$$

Collisions of the particles with the surface are assumed to be perfectly inelastic, such that all particles reaching the surface stay there.

The initial conditions (1.1) are written in dimensionless form

$$t = 0\colon\ \mathbf{U}_1 = \mathbf{U}_2 = 0,\ \rho_1 = \exp(-z/\mathrm{Eu}),\ p = \rho_1,$$
$$n = \exp\left[-(r^2 + (z - H)^2)\right],\ \rho_2 = M_{21}n, \tag{1.7}$$
$$H = H_0/R, \quad M_{21} = \pi d^3\rho_2^0 n_0/6\rho_{10},$$

where H is the dimensionless initial height of the cloud; M_{21} is the ratio of the initial mean density of particles at the center of the cloud to the initial gas density near the surface of precipitation. For a cloud of radius 1 m in air at normal conditions, $\mathrm{Re} \sim 10^5$, which corresponds to the generation of turbulence. We use a smoothed description of turbulent motion by introducing an effective turbulent viscosity (see pg. 292 of [5]). But the drag force of an individual particle is calculated using the molecular viscosity, since the quantity Re_p^0 is within the region of applicability of the empirical function for the drag coefficient used here (for example $\mathrm{Re}_p^0 \sim 10$ for a particle with d = 100 μm and the conditions described above). Hence Re and Re_p^0 are independent parameters.

The calculations were performed using the constant values $\mathrm{Eu} = 10^3$, Re = 30, $\mathrm{Re}_p^0 = 400$. The other parameters were varied within the following limits: $M_{21} = 0.01$-3, $\tau_r = 0.5$-2, H = 2-12.

The problem specified by (1.2) through (1.7) was solved numerically by a finite-difference method using the method of [6] for the equations of motion of the gas and the longitudinal–transverse scheme of [7] for the equations of motion of the particles. A nonuniform 20 × 40 grid was used with an increased density of grid points near the coordinate axes. The Courant number, constructed from the speed of sound and the minimum grid stepsize, was equal to 4. The execution time of a run was 2 to 3 hours on the ES-1055 computer. A detailed description of the numerical methods used can be found in [1, 8].

2. We consider first the evolution of the cloud up to the time at which the effect of the surface of precipitation begins to be felt (we assume an infinite medium). If the mass fraction of particles is large enough they can interact hydrodynamically through the carrier

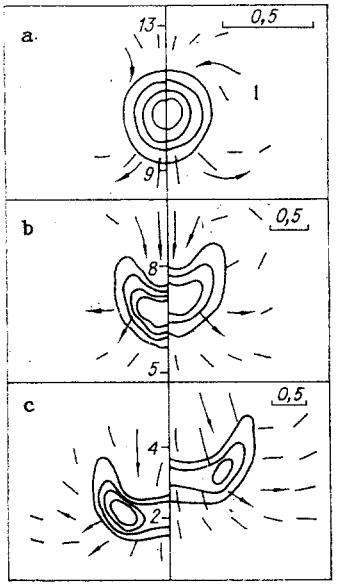

Fig. 1

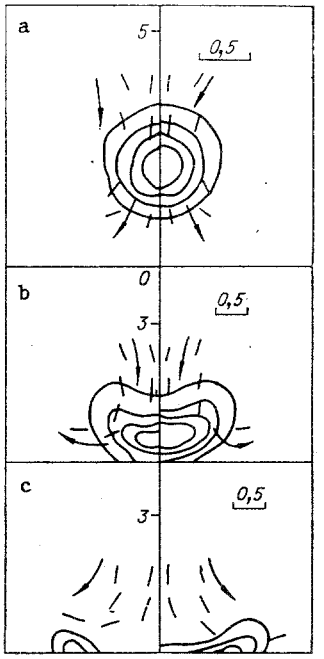

Fig. 2

medium. Gas is dragged downward by the falling particles and a large-scale vortex motion results. As a result, the rate of fall of the cloud of suspended particles exceeds the rate of fall of a single isolated particle in the same medium (the entrainment regime of the cloud). Since the degree of which the gas is dragged into the motion is determined by parameters which do not depend on the geometry of the problem, the range of parameters for which the entrainment regime is realized will be the same for the plane-symmetric and axisymmetric cases. This region of parameter space was determined by solving the plane-symmetric problem in [1, 2]. Below we consider only the entrainment regime, since motion of the cloud with small hydrodynamic interaction of particles (the filtration regime) reduces to finding the motion of a single particle, and was studied in detail in [9].

The evolution of the falling cloud of suspended particles is shown in Fig. 1 for the plane-symmetric and axisymmetric cases. Figure 1 shows the curves of equal concentration of particles in the cloud and the velocity vectors of the gas for a typical run ($M_{21} = 0.5$, $\tau_r = 1$) for the times t = 1.86; 13.96; 7.45 (curves a through c). Here, as in Fig. 2, the field for the axisymmetric problem is shown on the left and that for the plane-symmetric problem is shown on the right. The values of the concentration on neighboring contours differ by 0.2, and n = 0.2 on the outermost contour. The velocity scale is specified in the figures.

It is evident that the qualitative picture of the evolution is identical in the two cases: the downward motion of the particles causes a vortex motion, which at first transforms the cloud into a "bowl-like" shape (Fig. 1b) and then the cloud is drawn out along the horizontal, and hence the maximum concentration of particles is displaced from the axis (plane) of symmetry in the transverse direction (Fig. 1c). The initial cylindrical cloud breaks up into two symmetric parts (plane symmetry) and the initial spherical cloud condenses into a ring (axial symmetry). The distinguishing features of the axisymmetric case are the large rate of fall of the cloud and the sharper concentration gradient of particles in the cloud during its precipitation.

3. We consider now the precipitation of the cloud of particles on the horizontal surface. Typical examples of this process are shown in Fig. 2 for axial and plane symmetry, where the velocity field of the gas and the lines of constant concentration of particles of the precipitating cloud ($M_{21} = 0.3$, $\tau_r = 1$, H = 3.26) are shown at the times t = 3.41; 6.82; 10.22 (a through c). We see that precipitation proceeds in an identical way for the two cases. The vortex motion of the carrier medium induced by the motion of the cloud (a) drags along particles in the transverse directions (b, c), which leads to a scattering of particles along the surface of precipitation. As a result, in some cases the final distribution of surface concentration of precipitated particles has a local minimum at r = 0, and a significant fraction of particles fall outside of the region defined by the initial projection of the cloud onto

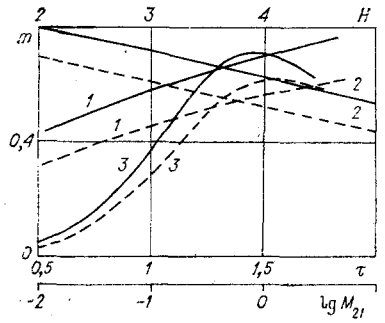

Fig. 3

the surface. This effect was treated quantitatively in [1, 2] by introducing a scattering coefficient for the cloud of particles equal to the fraction of particles falling outside of initial projection of the cloud onto the surface.

The dependence of the scattering coefficient on the parameters of the problem is shown in Fig. 3 for the plane-symmetric (dashed curves) and axisymmetric (solid curves) cases.

When the height of the cloud increases, the scattering of particles on the surface below also increases in both the plane-symmetric and axisymmetric cases (curve 1, $M_{21} = 1$, $\tau_r = 1$). The higher the initial height of the cloud, the greater the quantity of gas dragged into the induced vortex flow. Hence the transverse transport of particles is enhanced, and this increases their scattering.

An increase in the velocity relaxation time τ_r of a particle leads to a decrease in the scattering coefficient of the cloud of particles on the surface, independent of the symmetry of the problem (curve 2, $M_{21} = 1$, $H = 3.26$). This can be explained by the fact that the parameter τ_r characterizes the "coupling" of the phases; the smaller this quantity, the more rapidly the particles are carried along by the carrier medium.

The dependence of the scattering coefficient on the parameter M_{21}, which is proportional to the initial concentration of particles in the cloud, shows a maximum. The maximum is pronounced for the axisymmetric case (curve 3 with $\tau_r = 1$, $H = 3.26$). For small values of M_{21} the cloud collapses in a manner similar to the filtration regime. In this case the scattering coefficients of the cloud are quite small for both geometries and differ from one another insignificantly. When the concentration of particles increases, their hydrodynamic interaction also increases, and this leads to large-scale vortex motion as the cloud falls. Hence the scattering coefficient increases. When the concentration of particles is increased further ($M_{21} \gtrsim 1$) the rate of fall of the cloud becomes so large that the induced vortex flow becomes incapable of transporting particles in a significant distance in the transverse direction and the scattering of particles begins to decrease.

We note that the scattering of particles is larger in the axisymmetric case than in the plane-symmetric case, for the same parameters of the cloud. For the ranges of the parameters considered here, the largest difference in the scattering coefficients is 0.1. Our study shows that it is possible to approximately convert theoretical and experimental data on the precipitation of a spherical cloud to the precipitation of a cloud in the plane-symmetric case, and vice versa. Here it is necessary to satisfy the similarity criteria introduced above.

The author thanks A. N. Kraiko for useful discussions.

LITERATURE CITED

1. G. M. Makhviladze and O. I. Melikhov, "Numerical study of the falling of a group of monodispersed particles onto a plane horizontal surface" [in Russian], Preprint, Inst. Problems of Mechanics, Academy of Sciences of the USSR, No. 191, Moscow (1981).
2. G. M. Makhviladze and O. I. Melikhov, "On the motion of a group of particles under gravity and precipitation onto a plane horizontal surface," Izv. Akad. Nauk, Mekh. Zhidk. Gaza, No. 6 (1982).
3. A. L. Dorfman, "Numerical study of two-phase flow in a viscous carrier phase," Izv. Akad. Nauk, Mekh. Zhidk. Gaza, No. 3 (1981).
4. R. I. Nigmatulin, Foundations of the Mechanics of Heterogeneous Media [in Russian], Nauka, Moscow (1978).

5. A. S. Monin and A. M. Yaglom, Statistical Hydromechanics. Mechanics of Turbulence [in Russian], Fizmatgiz, Moscow (1965), Ch. 1.
6. G. M. Makhviladze and S. B. Shcherbak, "Numerical study of the motion of a compressible gas," Inz.-Fiz. Zh., 38, No. 3 (1980).
7. A. A. Samarskii, Theory of Difference Schemes [in Russian], Nauka, Moscow (1977).
8. G. M. Makhviladze and O. I. Melikhov, "Large-scale vortex motion in the falling and precipitation of a group of monodispersed particles," ChMMSS, 13, No. 4 (1982).
9. N. A. Fuks, Mechanics of Aerosols [in Russian], Academy of Sciences of the USSR, Moscow (1955).

STRUCTURE OF A COMPRESSION SHOCK IN TWO-PHASE MEDIA

A. M. Grishin and G. G. Tivanov

UDC 532.529:518.5

Shockwaves originating in supersonic two-phase flows can be considered to consist of two zones – the compression shock that is realized at the shock velocity greater than the frozen speed of sound [1, 2], and the relaxation zone. Although the structure of the relaxation zone has been investigated in sufficient detail [1-5], the structure of the compression shock has not.

It is generally understood that a lifting medium is described by Hugoniot relationships during passage through a shock, while particles "ignore" the compression shock. Meanwhile, experimental data [3] display a sufficiently strong influence of the compression shock on heterogeneous inclusions if the particle size does not exceed 20-25 μm.

For sufficiently intensive shocks, shocks originate in the domain with as large as a two-phase medium flows around a solid boundary, where the stream parameters change substantially within distances commensurate with the dimensions of the inclusions. Models of a continuous medium do not hold in these zones and the structure of such flows can be investigated only within the framework of kinetic theory [6]. On the other hand, for a weak shock intensity the thickness of the compression shock can exceed the dimensions of the inclusions by an order and more, which permits utilization of the approximation of a continuous medium to investigate the compression shock structure.

Here we consider the structure of a compression shock by using the kinetic and hydrodynamic descriptions of a two-phase medium. It is shown that the presence of particles results in an increase in the compression shock thickness, where the particles exert the greatest influence on the density and velocity profiles. It is found that taking account of the dissipative components on both the kinetic and the hydrodynamic level broadens the limits of applicability of these approaches somewhat.

1. Since a compression shock especially influences fine particles, for simplicity in our analysis we shall henceforth limit ourselves to a study of small size inclusions (not more than 10 μm, for instance), which permits utilization of the diffusion approximation in individual cases.

We consider a two-phase medium as a dynamic system of interacting particles. We write the kinetic equations for the particles of each phase (subscripts i, j) in the form

$$Df_i/Dt = Q(f_i, f_j). \tag{1.1}$$

Here Q is the interaction integral, and f(t, $\mathbf{x}$, $\mathbf{v}$) is the particle distribution function of one phase.

Two interaction scales, short-range and sliding collisions, can be separated for an analysis of Q in application to a two-phase mixture [7]. For the short-range collision, direct contact occurs between two (or more) particles with an exchange of mass, momentum, and energy.

Tomsk. Translated from Zhurnal Prikladnoi Mekhaniki i Tekhnicheskoi Fiziki, No. 2, pp. 101-108, March-April, 1987. Original article submitted February 12, 1986.

